17th World Conference on Earthquake Engineering, 17WCEE
Sendai, Japan - September 13th to 18th 2020

BASE ISOLATION OF A MASONRY BUILDING USING MODIFIED RECTANGULAR FIBER-REINFORCED ELASTOMERIC ISOLATORS

S. Prakash[1], S. Ghodke[2], R. S. Jangid[3]

[1] *Doctoral Student, Indian Institute of Technology Bombay, shiv.prakash@iitb.ac.in*
[2] *Senior Research Associate, Indian Institute of Technology Bombay, ghodkesl@iitb.ac.in*
[3] *Professor, Indian Institute of Technology Bombay, rsjangid@civil.iitb.ac.in*

Abstract

This study focuses on the development and performance improvement of Unbonded Fiber-reinforced Elastomeric Isolators (U-FREI). Modified Rectangular U-FREIs are used to isolate a typical masonry building in India. A specific design procedure for modified rectangular isolators is proposed. Two configurations of a typical masonry building designed as per Indian Standard Codes are considered i.e. Fixed base and Base isolated using the isolators designed using the proposed method. Nonlinear time-history analysis is carried out using SAP2000 v20 [1]. Masonry is modeled as a homogenous material based on the analytical curves proposed in previous studies. Walls are modeled using the layered shell area element which assumes the membrane and plate bending behavior separately. Isolators are modeled as a combination of nonlinear spring and linear viscous damper in the software using the Backbone Curve model. Earthquake ground motions are selected for two hazard levels i.e. Maximum Considered Earthquake (MCE) having 2500-year return period and Design Based Earthquake (DBE) having 500-year return period. Site-specific uniform hazard response spectra using Probabilistic Seismic Hazard Analysis study of Ukhrul district in the Manipur state of India is used as the target spectra. A significant improvement in performance parameters i.e. base shear, peak floor acceleration and inter-story drift was seen in case of isolated structures as compared to those in fixed base structure proving the efficiency of isolation system and proposed design procedure. This will help in the development of a cost-effective and innovative base isolation system for masonry buildings in earthquake prone regions of the developing countries.

Keywords: Base Isolation; Modified rectangular fiber-reinforced elastomeric isolators; SAP2000; Masonry buildings

© The 17th World Conference on Earthquake Engineering

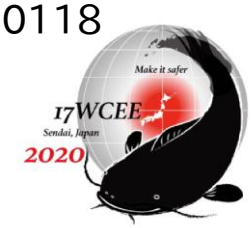

1. Introduction

Base isolation has long been used in bridges and buildings for seismic isolation. It is a passive mechanism based on low horizontal stiffness and high damping characteristics. Being cost-effective and seismically efficient, it has a lot of scope for its application in low and medium rise buildings in earthquake-prone regions of developing countries. Base isolators are widely classified into two types, namely sliding type and elastomeric bearing type. Elastomeric bearings are made of alternating layers of elastomeric polymer and reinforcement sheets. Natural rubber or neoprene pads are primely used as elastomeric polymer and steel plates or fiber layers are used as reinforcements. When steel shims are used as reinforcement in isolator then it's called steel-reinforced elastomeric isolators (SREI) and vice-versa in case of fiber (FREI). Kelly first evaluated the feasibility and mechanical properties (vertical stiffness etc.) of fiber as reinforcement in place of steel plates [2]. Using fiber layers as the reinforcement decreases the weight and manufacturing cost of the product as compared to SREIs. The high cost in the latter case comes due to high installation and manufacturing costs. Another factor which helps in cost reduction is use of cold vulcanizing products like rubber cement instead of hot vulcanization for bonding the elastomer and reinforcement layers. Steel shims being rigid in flexure, also put a high strength demand on the bond between the elastomer and reinforcement. This does not happen in case of FREIs due to lack of flexural rigidity in fiber layers [3–5]. When the FREI is bonded to the superstructure and substructure using steel end plates then it's called Bonded FREI otherwise Unbonded FREI (U-FREI). U-FREI shows a weight and cost improvement due to removal of end plates. Apart from this, an improvement in seismic efficiency is also seen in the case of U-FREIs due to a unique phenomenon known as "Rollover". In Rollover phenomenon, as the horizontal displacement increases initially, the area in contact with the superstructure and substructure decreases, due to which the horizontal stiffness decreases. Horizontal displacement keeps on increasing till the vertical surfaces of the isolator start touching the upper and lower supports. This state is known as "Full Rollover". Further increase in horizontal displacement will cause an increase in horizontal stiffness which will work as a displacement check to prevent the structure from overturning or being unstable [6]. The excessive displacement before the isolator reaches the full rollover can be controlled by using elastomer with high damping capacity.

Most of the isolators being used today are square or circular in shape. Square or circular isolators are generally placed under the columns in case of framed structures. In case of building with masonry and structural walls, a wall beam is needed underneath the structure and above the isolators for a uniform support under the superstructure. If a rectangular strip isolator is used in place of square or circular isolators, the reinforcement need in wall beams can be reduced, or these beams can be removed altogether [2, 7]. As isolators become more rectangular, its aspect ratio increases along the longer direction. This increased aspect ratio causes an increase in horizontal stiffness along the longer (loading) direction, which further decreases the shift in the period of structure thus decreasing the isolation efficiency. To overcome this difficulty, modifications like holes are introduced in the isolators. Van Ngelen [8] first introduced the idea of introduction of holes and studied its effects on the horizontal behavior of the isolator. Lower horizontal stiffness at intermediate displacements and higher stiffness at higher displacements was found which confirmed the effectiveness of modification i.e. holes. Introduction of holes also increases the compressive stress thus improving the lateral behavior of isolators [9]. These modified isolators are called Modified Rectangular Unbonded Fiber-reinforced Elastomeric Isolators (MR-UFREI). Compression behavior of MR-UFREI showed an increase in vertical stress and tensile stress in elastomer and fiber layers respectively in the vicinity of modifications [10]. Though some preliminary investigation of MR-UFREI's behavior has been done in the studies discussed above, still it's design, behavior and efficiency under real ground motions for a masonry building is still unknown. Square or circular UFREI have same behavior along both direction which is not the case with rectangular FREI. Thus, the design procedure of rectangular UFREI or MR-UFREI will be different and needs separate formulation.

In this study, a design procedure for MR-UFREI is proposed first. Isolators (MR-UFREI) are designed using the aforementioned design procedure for a typical masonry building in India designed as per Indian Standards. A nonlinear time-history analysis of the designed building in both fixed base (FB) and base isolated (BI) condition is done in SAP2000 [1]. The efficiency of the isolation system is investigated by comparing the various seismic response parameters in both configurations.

© The 17th World Conference on Earthquake Engineering

2. Methodology

2.1 Building Specifications and Modelling

A typical masonry building commonly found in rural and semi-urban areas of India was designed as per IS 1905-1987 [11, 12]. The building's plan view with symmetric placement of isolators is shown in Fig.1. The building has three stories of height three meters each. As the study is about the relative behavior of a base-isolated and fixed base buildings and thus comparative, some basic omissions like doors and windows have been made. Normally in these buildings, doors and window dimensions are small and situated near center thus avoiding any column effect in the walls. The building consists of load-bearing masonry walls of thickness 200 mm supporting the RCC floor slabs and roof slabs of thickness 150 mm and 100 mm respectively. The loading combinations were taken as per IS code specifications [13, 14].

The mortar grade obtained after design was H2 (Cement: Lime: Sand = 1: 0.5: 4.5) with brick size of 230 mm × 115 mm × 75 mm having crushing strength of 5 MPa. Roof and floor slabs were modeled using shell element and walls were modeled using layered nonlinear shell element. Rigid diaphragms were assumed at all floors for simplicity. The stress-strain relationships of the masonry were adopted from Refs. [15–18]. The resulting in-plane axial and shear stress-strain plots are shown in Fig.2 and Fig.3 respectively.

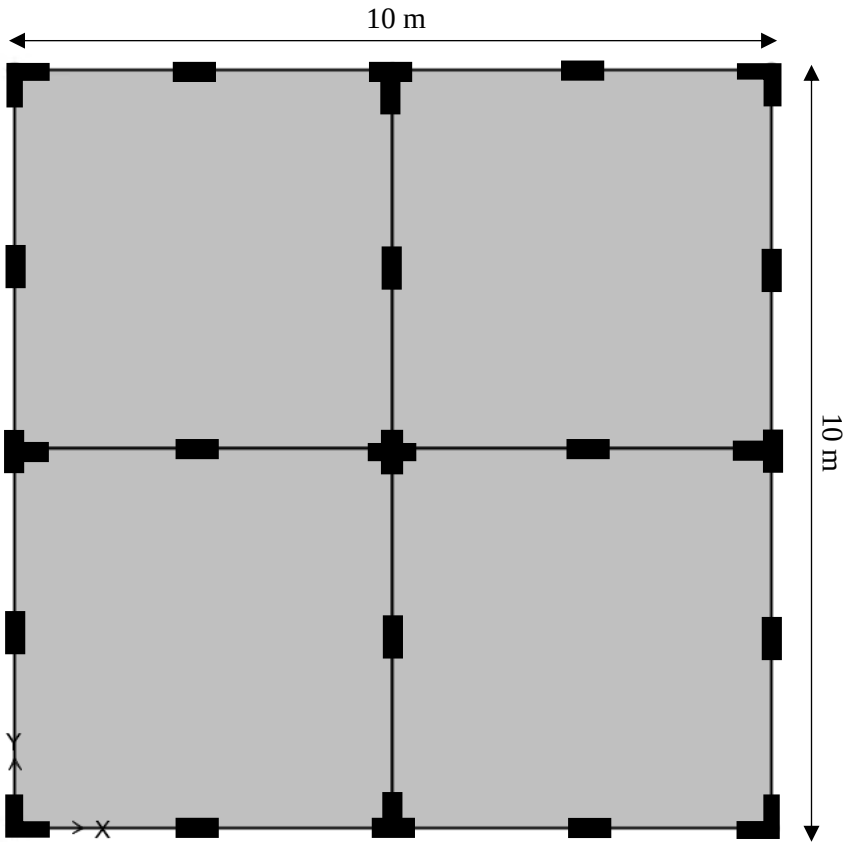

Figure 1 – Plan view of building (■ = isolator, not to scale)

© The 17th World Conference on Earthquake Engineering

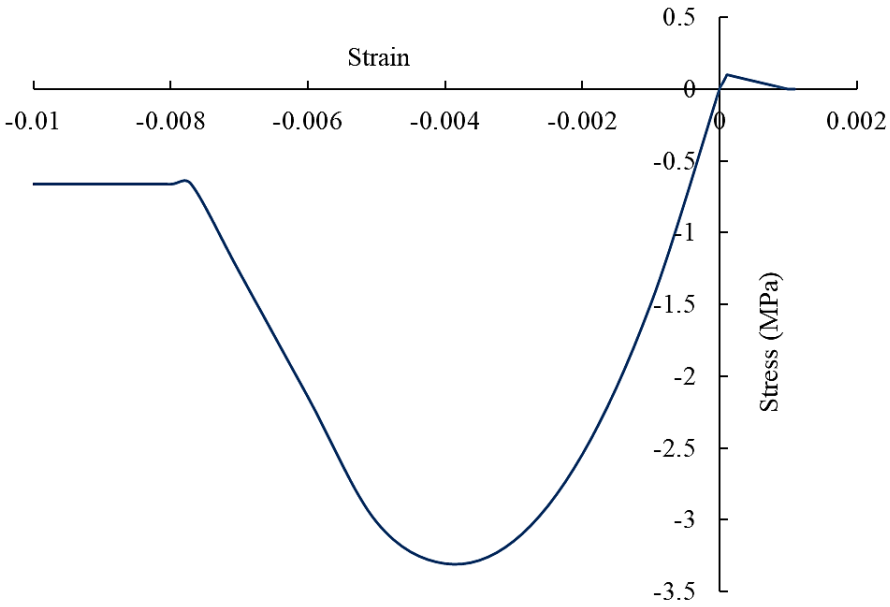

Figure 2 – Masonry axial stress-strain plot

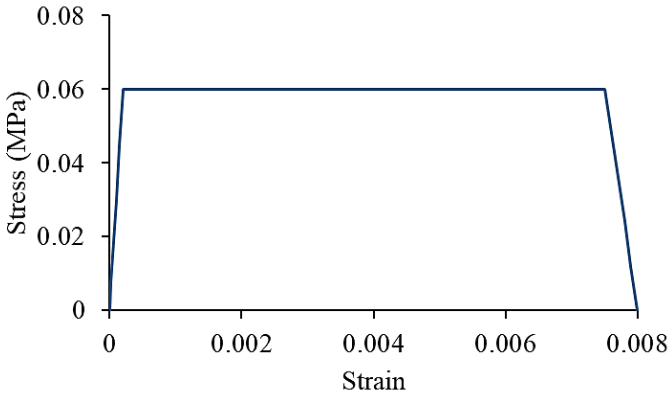

Figure 3 – Masonry Shear stress-strain plot

2.2 Earthquake Selection

A Probabilistic Seismic Hazard Analysis (PSHA) study for Ukhrul district in Manipur, India was adopted for finding the design-based response spectra [19]. Two hazard levels have been considered: Maximum Considered Earthquake (MCE) having 2500-year return period and Design Based Earthquake (DBE) having 500-year return period. The response spectra for both hazard level and also for Standard Level Earthquake (SLE) having 100-year return period is given in Fig.4. PEER-NGA database was used to find the ground motions for time-history analysis [20]. As per ASCE/SEI 7-10, 2013 [21], 10 ground motions were selected by minimizing the least square error between mean response spectra and target spectra for the time period (T) range, $0.5T_F$ to $1.25T_M$. T_F is time-period of fixed base (FB) structure and is found using the structural model and T_M is the time-period of base isolated (BI) structure which comes out to be 1.73 s from isolator design. Thus, spectral matching is done from $T = 0.5T_F$ to $T = 1.25T_M$. The spectral matching procedure for DBE

© The 17th World Conference on Earthquake Engineering

hazard level is shown in Fig.5. For simplicity, the ground motions obtained for DBE level hazard case is multiplied by 1.5 and 0.5 to get the ground motion data for MCE and SLE case as per ASCE/SEI 7-10, 2013 [21].

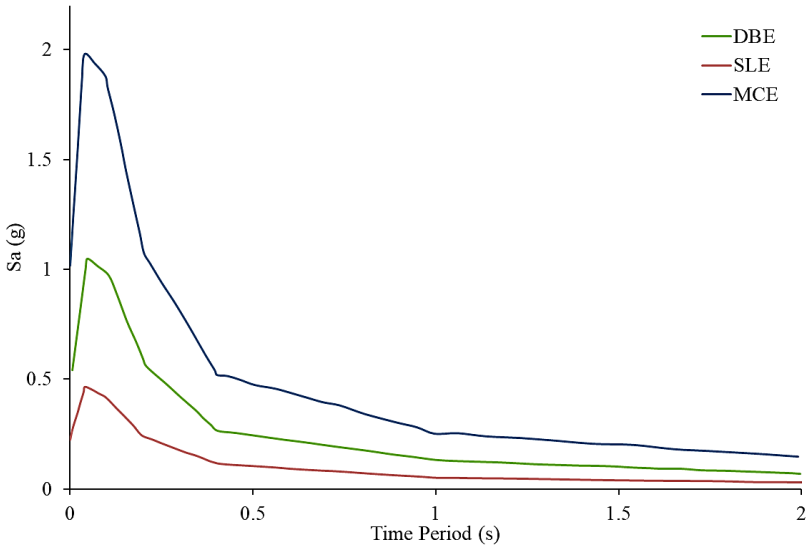

Figure 4 – Response Spectra

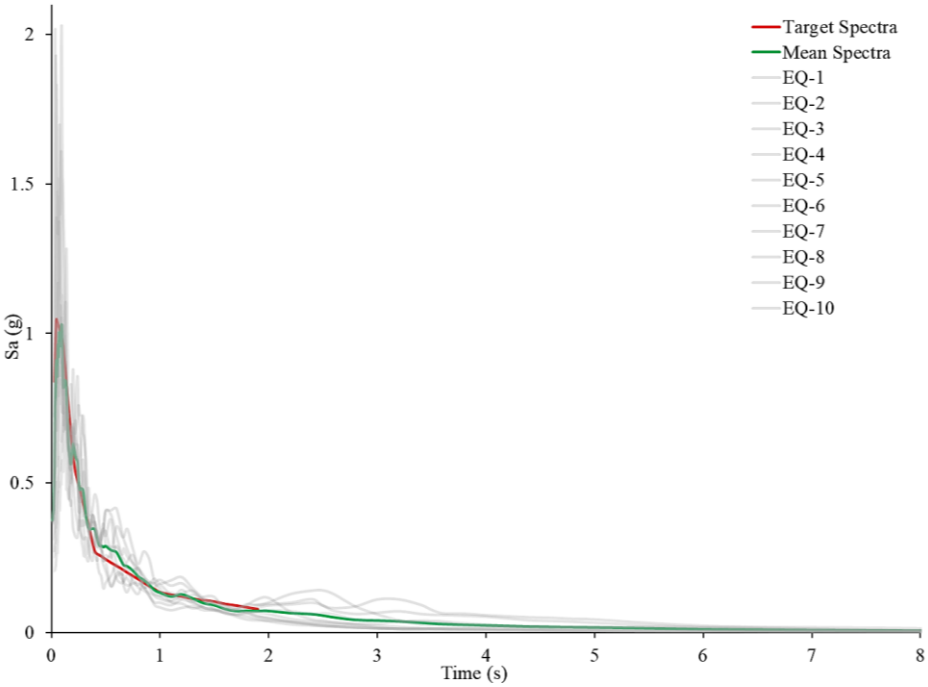

Figure 5 – Spectral Matching Result

© The 17th World Conference on Earthquake Engineering

2.3 Isolator design

A design procedure for MR-UFREIs was proposed based on previous studies done in this area and the provisions of ASCE/SEI 7-10, 2013 [21]. The design procedure is shown in Fig.6 which is modified and adapted for MR-UFREIs from the works done by Refs. [22, 23]on U-FREI's. This same procedure can also be used for design of unmodified rectangular FREIs by taking x (modification percentage) = 0 in Fig.6. Step 1 begins with assuming the range for initial parameters based on the data from previous studies [21, 22] and from current industrial practices

$$0.4 \text{ MPa } (G_{min}) \leq G \text{ (Shear Modulus)} \leq 0.9 \text{ MPa } (G_{max})$$

$$15 \ (S_{min}) \leq S \text{ (Shape Factor)} \leq 20 \ (S_{max})$$

$$1 \text{ MPa } (p_{min}) \leq p \text{ (Vertical Pressure)} \leq 3 \text{ MPa } (p_{max})$$

Plan area with modification (A_{in}) is calculated using the pressure (p) and weight (w) coming on each isolator. Then as per designer's choice for x, the dimensions of the isolator i.e. b, a and h are calculated. Now, based on the structure and its FB time period T_F, time-period of the isolator is taken in the range of $3T_F$ to 3s [22]. In Step 2 of the procedure, the maximum displacement of isolator under MCE level earthquake (D_M) is calculated using [21]. As the isolator's efficiency is maximum when shear strain is more than hundred percent but less than the full rollover displacement, a check is introduced at this step [23]. Full rollover happens at early displacements for MR-UFREI's thus a lower value of full-rollover displacement is taken [24]. This value can be further improved by investigating the effect of modifications on full-rollover displacement. Now, if the isolator fails the check, it goes back to Step 1 with improved initial parameters otherwise it goes to Step 3. As the behavior of an individual rectangular isolator in both orthogonal directions will not be same, hence the isolators are designed in pairs, perpendicularly placed to each other. Thus, effective area (A_{eff}) and effective stiffness (k_M) is found for each pair in Step 3 of the design procedure [25]. A constant effective shear modulus is taken for elastomer while calculating the effective stiffness for simplicity. Other specifications of the isolators i.e. t_f (Fibre-layer thickness), n (number of elastomer layers), t (Elastomer Layer thickness), t_{cover} (Elastomer cover layer thickness), t_r (Total thickness of Elastomer) are also found in this step. The second isolated time-period (T_{M2}) is calculated and compared with initial time-period, T_M. If the difference is between the tolerance limits then it exits with that time-period else it goes back to Step 2 with new time period, T_{M2}.

After carrying out the design of the isolators, total number of isolators required for the structure was found to be 30. Half of the isolators were placed longitudinally along a wall direction and the rest half along the perpendicular wall direction for a symmetric layout (Fig.1). The dimension of the designed isolator was 425.63 mm × 195.8 mm × 85.13 mm. Thirteen inner elastomer layers of thickness 5.36 mm each and two outer layers of thickness 2.68 mm each were taken. Shear modulus of elastomer was taken as 0.4 MPa. Fourteen layers of Carbon fiber of thickness 0.55 mm each was used alternatively after every elastomer layer. A circular hole of radius 72.835 mm was made in center thus reducing the plan area by 20%. Isolated time period came out to be 1.73 s.

2.4 Isolator Modelling

The isolator's behavior is simplified using the Backbone curve model for modelling it in SAP2000 [1]. This model is a combination of a Linear Viscous Damper and Nonlinear Spring Element. The parameters of the model are found by minimizing the least square error between the finite element (FE) response obtained during the application of displacement boundary condition with those predicted by the model. The stiffness and damping forces with displacement 'u' is calculated as

$$F_T = F_{spring} + F_{dashpot} \quad (1)$$

$$F_{spring} = a_1 + a_2u^3 + a_3u^5 \quad (2)$$

© The 17th World Conference on Earthquake Engineering

$$F_{\text{dashpot}} = C\dot{u} = 2\beta_{\text{eff}}\sqrt{(mk_{\text{eff}})} \quad (3)$$

Here a_i are the coefficients and C is damping constant related to m, k_{eff} and β_{eff} which are mass, effective stiffness and effective damping respectively. The FE response was found using a commercial FE- software, ANSYS 16.2 [26]. Isolators were modeled and analyzed under a constant vertical load and sinusoidal displacement boundary conditions at different amplitudes and stiffness and damping values were calculated. Ogden model parameters and Prony series from Refs. [27, 28] was used to model the hyperplastic and viscoelastic behavior of rubber. The Finite Element (FE) model verification was done using the results obtained in other previous FE-studies of isolators [3, 5, 29].

Modal parameters (Table 1) corresponding to five displacement amplitudes i.e. $0.25t_r$, $0.5t_r$, $0.75t_r$, $1.0t_r$ and $1.25t_r$ were calculated using the FE data (t_r is the total height of elastomer in the isolator). A combination of Multilinear Spring and Linear Viscous link elements were used to model the isolator's behavior.

Table 1 – Backbone Curve model parameters

Displacement Amplitude, t_r	**Direction**	**a_1/(GA/t_r)**	**a_2/(GA/t_r^3)**	**a_3/(GA/t_r^5)**	**C/GA**
0.25	Longitudinal	1.478995	3.16E-06	-9.83E-10	0.001712
	Transverse	1.36301	2.73E-06	-8.14E-10	0.001679
0.5	Longitudinal	1.414626	6.94E-07	-5.07E-11	0.001703
	Transverse	1.257342	5.45E-07	-3.64E-11	0.001637
0.75	Longitudinal	1.340524	2.87E-07	-8.94E-12	0.001716
	Transverse	1.143994	2.07E-07	-5.65E-12	0.00164
1	Longitudinal	1.278264	1.51E-07	-2.53E-12	0.001746
	Transverse	1.042013	1.00E-07	-1.35E-12	0.001656
1.25	Longitudinal	1.183841	9.37E-08	-9.77E-13	0.001818
	Transverse	0.942272	5.56E-08	-4.05E-13	0.001691

2.5 Nonlinear Time-History Analysis

An iterative procedure was used for the time history analysis of the BI structure under the selected earthquake ground motions. Firstly, the analysis was run using the Backbone curve parameters corresponding to each displacement amplitudes for each of the ground motions. Maximum displacement was calculated during each run. Secondly for each ground motion, the error between the maximum displacement obtained during the time-history analysis and the displacement amplitude for which the parameters were taken was calculated at all displacement amplitudes. Then in final run, parameters having minimum error was selected for each ground motion. Direct integration approach and Hilbert-Hughes-Taylor method were used for nonlinear time history analysis. Final response was taken as an average of the responses obtained against all the 10 ground motions.

© The 17th World Conference on Earthquake Engineering

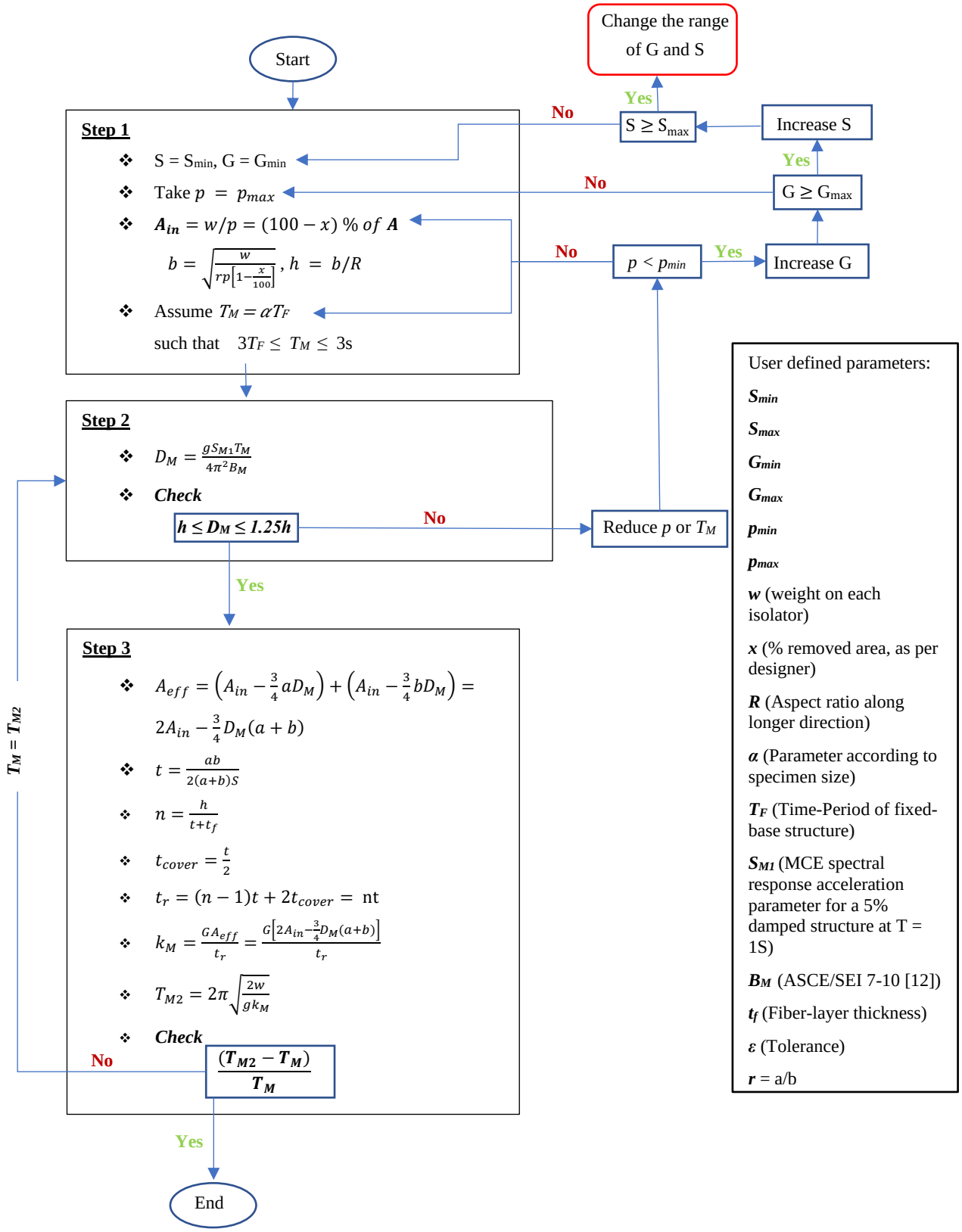

Figure 6 – Flow chart of the MR-UFREI design procedure

© The 17th World Conference on Earthquake Engineering

3. Results and Discussion

Results showed that the MR-UFREI's low stiffness and high damping behavior successfully improved the seismic performance of the structure. The first three modes of the BI structure were rigid body modes. Time period of the BI structure fell short of the designed time period but still increased by 4.45 times that of the FB structure. This difference be further minimized by using more refined horizontal stiffness formulations of U-FREI. The major seismic response parameters were calculated from the analysis results. High floor acceleration and Inter-story drift are one of the major causes of the structural and non-structural damages to the masonry buildings in earthquake affected areas. As Maximum Floor acceleration for MCE-level earthquake will always be higher than DBE-level so a ratio of Peak Floor Acceleration (PFA) and Peak Ground Acceleration (PGA) is calculated to quantify the variation. Plot of the PGA/PFA variation with floor level is given in the Fig.7.

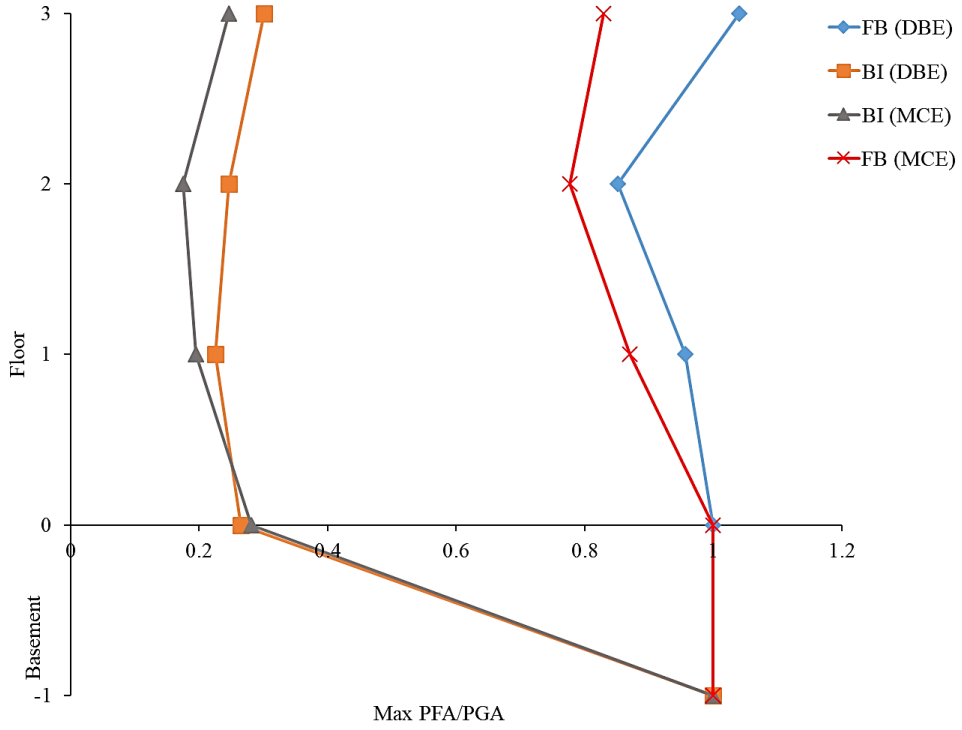

Figure 7 – Maximum PFA/PGA of different floors

A significant improvement in the above-mentioned ratio is seen in the base-isolated case as compared to fixed-base case. The decrease in PFA/PGA ratio were higher in topmost and ground floor as compared to middle floors. Similar behavior is again observed in case of Inter-story drift. Here inter-story drift was measured in terms of Inter-story Drift Ratio (IDR) which is the relative displacement of two floors divided by the floor height. As shown in Fig.8, IDR was found higher in lower floors in case of BI structure, while in case of FB structure, it first increases and then decreases with floor level. Higher IDR values in lower floors in case of FB structures can be attributed to the fixed nature of the base nodes of the building. Lower IDR values in BI case showed the near-rigid behavior of the structure. Thus, base isolation has successfully managed to decrease the Inter-story drift by a significant amount. Base shear reduction was approximately 63% in case of the isolate base as compared to FB case. Base-isolated response results obtained are shown in Table 2. Maximum displacement in isolator was also way below than the full-rollover displacement. Maximum displacement was calculated for each earthquake and both hazard levels and accordingly the final parameters of the isolators were selected.

© The 17th World Conference on Earthquake Engineering

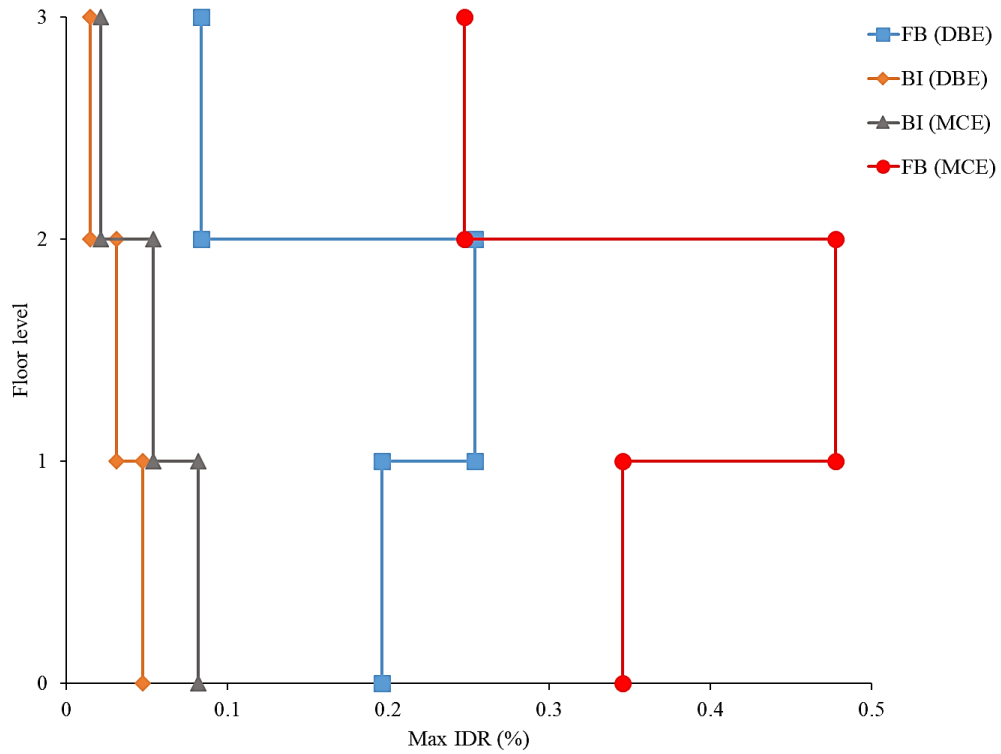

Figure 8 – Maximum Inter-story Drift Ratio

Table 2 – Base Isolated response results

Hazard Level		**DBE**	**MCE**
Time Period *(1st Mode)*		1.35 s	1.38 s
Base Shear *(normalized w.r.t FB response)*		0.37	0.386
Maximum IDR *(normalized w.r.t FB response)*	1st Floor	0.24	0.24
	2nd Floor	0.12	0.11
	3rd Floor	0.18	0.087
Maximum PFA/PGA *(normalized w.r.t FB response)*	Ground Floor	0.265	0.26
	1st Floor	0.225	0.22
	2nd Floor	0.246	0.23
	3rd Floor	0.3	0.28

© The 17th World Conference on Earthquake Engineering

4. Conclusion

A design procedure for MR-UFREIs is proposed in this paper for isolation of masonry buildings. Isolators being rectangular in plan has different behavior in orthogonal directions and thus were designed in pairs. Further, the efficiency of the design procedure and isolation system was investigated by a comparative study of the nonlinear time-history response of the fixed-base and base-isolated version of a typical masonry building in India under a set of chosen ground motions. Modal response showed that the first three modes in base-isolated case were dominated by isolation system. Time-history analysis showed significant improvements in various response parameters i.e. base shear, floor acceleration and inter-story drift. Despite a significant increase in time period (4.45 times) in BI case, it fell short of the designed isolated period. This difference can be further reduced by using a more refined horizontal stiffness formulation of U-FREI. Though the design procedure proposed in the study is for MR-UFREI but it can also be used for any rectangular unmodified/modified U-FREI by taking the full rollover displacement and modification percentage accordingly. It is expected that this study will help with the necessary steps required for the design of rectangular U-FREI in case of masonry buildings.

Future scope includes the investigation of the end buckling and damping characteristics of the MR-UFREI by real-scale testing as introduction of holes leaves the rest ends along the shorter edge susceptible to buckling and also affects the damping.

References

[1] SAP2000, C. S. I. (2018). v20 Integrated Finite Element Analysis and Design of Structures. *Computers and Structures Inc.: Berkely, CA, USA*.

[2] Kelly, J. (1999). Analysis of Fiber-Reinforced Elastomeric Isolators. *Journal of Seismology and Earthquake Engineering*.

[3] Toopchi-Nezhad, H., Tait, M. J., & Drysdale, R. G. (2011). Bonded versus unbonded strip fiber reinforced elastomeric isolators: Finite element analysis. *Composite Structures*, *93*(2), 850–859. https://doi.org/10.1016/j.compstruct.2010.07.009

[4] Habieb, A. B., Milani, G., & Tavio, T. (2018). Two-step advanced numerical approach for the design of low-cost unbonded fiber reinforced elastomeric seismic isolation systems in new masonry buildings. *Engineering Failure Analysis*, *90*, 380–396. https://doi.org/10.1016/j.engfailanal.2018.04.002

[5] Das, A., Dutta, A., & Deb, S. K. (2015). Performance of fiber-reinforced elastomeric base isolators under cyclic excitation. *Structural Control and Health Monitoring*, *22*(2), 197–220. https://doi.org/10.1002/stc.1668

[6] Crozier, W. F., Stoker, J. R., Martin, V. C., & Nordlin, E. F. (n.d.). *BRIDGE BEARING PADS*. 55–58.

[7] Kelly, J. M. (2002). Seismic Isolation Systems for Developing Countries. *Earthquake Spectra*, *18*(3), 385–406. https://doi.org/10.1193/1.1503339

[8] Van Engelen, N. C., Tait, M. J., & Konstantinidis, D. (2012). Horizontal Behaviour of Stable Unbonded Fiber Reinforced Elastomeric Isolators (SU-FREIs) with Holes. *15th World Conference on Earthquake Engineering*, *Kelly 1999*.

[9] de Raaf, M. G. P., Tait, M. J., & Toopchi-Nezhad, H. (2011). Stability of fiber-reinforced elastomeric bearings in an unbonded application. *Journal of Composite Materials*, *45*(18), 1873–1884. https://doi.org/10.1177/0021998310388319.

[10] Van Engelen, N. C., Osgooei, P. M., Tait, M. J., & Konstantinidis, D. (2014). Experimental and finite element study on the compression properties of Modified Rectangular Fiber-Reinforced Elastomeric Isolators (MR-FREIs). *Engineering Structures*, *74*, 52-64.

[11] Bureau of Indian Standards (BIS). (1987). IS 1905-1987: Code of Practice for Structural use of Unreinforced Masonry. In *Indian Standards*.

[12] Sinha, R., & Brzev, S. N. (2002). Unreinforced brick masonry building with reinforced concrete roof slab. In *World*

© The 17th World Conference on Earthquake Engineering

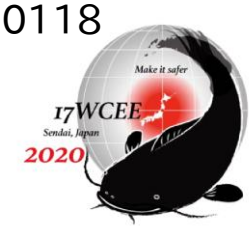

Housing Encyclopedia (pp. 1–15). http://www.world-housing.net/WHEReports/wh100054.pdf

[13] IS 875 : 1987. (1987). Code of Practice for Design Loads (Other than Earthquake) for Buildings and Structures, Part 2: Imposed Loads. *Bureau of Indian Standards, New Delhi*.

[14] Bureau of Indian Standard(BIS). (1992). Common Burnt Clay Building Bricks. *Is 1077*.

[15] Akhaveissy, A. H., & Milani, G. (2013). Pushover analysis of large scale unreinforced masonry structures by means of a fully 2D non-linear model. *Construction and Building Materials*. https://doi.org/10.1016/j.conbuildmat.2012.12.006

[16] Kaushik, H. B., Rai, D. C., & Jain, S. K. (2007). Uniaxial compressive stress-strain model for clay brick masonry. *Current Science*, *92*(4), 497–501.

[17] Sharma, A., & Khare, R. (2016). Pushover Analysis for Seismic Evaluation of Masonry Wall. *International Journal of Structural and Civil Engineering Research*, *5*(3), 235–240. https://doi.org/10.18178/ijscer.5.3.235-240

[18] Korini, O., & Bilgin, H. (2012). A new modeling approach in the pushover analysis of masonry structures. *International Students' Conference of Civil Engineering, ISCCE 2012*, *May*, 1–8.

[19] Pallav, K., Raghukanth, S. T. G., & Singh, K. D. (2012). Probabilistic seismic hazard estimation of Manipur, India. *Journal of Geophysics and Engineering*, *9*(5), 516–533. https://doi.org/10.1088/1742-2132/9/5/516

[20] Goulet, C. A., Kishida, T., Ancheta, T. D., Cramer, C. H., Darragh, R. B., Silva, W. J., ... & Youngs, R. R. (2014). Peer nga-east database. PEER Report 2014, 17.ASCE/SEI 7-10. (2013). *Minimum Design Loads for Buildings and Other Structures*. American Society of Civil Engineers. https://doi.org/10.1061/9780784412916

[21] ASCE/SEI 7-10. (2013). *Minimum Design Loads for Buildings and Other Structures*. American Society of Civil Engineers. https://doi.org/10.1061/9780784412916

[22] Ehsani, B., & Toopchi-Nezhad, H. (2017). Systematic design of unbonded fiber reinforced elastomeric isolators. *Engineering Structures*, *132*, 383–398. https://doi.org/10.1016/j.engstruct.2016.11.036

[23] Pauletta, M. (2019). Method to design fiber-reinforced elastomeric isolators (U-FREIs) and application. *Engineering Structures*, *197*(July). https://doi.org/10.1016/j.engstruct.2019.109366

[24] Osgooei, P. M., Van Engelen, N. C., Konstantinidis, D., & Tait, M. J. (2015). Experimental and finite element study on the lateral response of modified rectangular fiber-reinforced elastomeric isolators (MR-FREIs). *Engineering Structures*, *85*, 293–303. https://doi.org/10.1016/j.engstruct.2014.11.037

[25] Toopchi-Nezhad, H. (2014). Horizontal stiffness solutions for unbonded fiber reinforced elastomeric bearings. *Structural Engineering and Mechanics*, *49*(3), 395–410. https://doi.org/10.12989/sem.2014.49.3.395

[26] APDL, A. M. (2015). Release 16.2. ANSYS Inc., Canonsburg, PA.

[27] Ogden, R. W. (1972). Large Deformation Isotropic Elasticity - On the Correlation of Theory and Experiment for Incompressible Rubberlike Solids. *Proceedings of the Royal Society A: Mathematical, Physical and Engineering Sciences*, *326*(1567), 565–584. https://doi.org/10.1098/rspa.1972.0026

[28] Holzapfel, G. A. (1996). On large strain viscoelasticity: Continuum formulation and finite element applications to elastomeric structures. *International Journal for Numerical Methods in Engineering*, *39*(22), 3903–3926. https://doi.org/10.1002/(SICI)1097-0207(19961130)39:22<3903::AID-NME34>3.0.CO;2-C

[29] Ngo, T. Van, Dutta, A., & Deb, S. K. (2016). *Predicting stability of a prototype un-bonded fibre-reinforced elastomeric isolator by finite element analysis*. 1–23.

© The 17th World Conference on Earthquake Engineering